PERGAMON

International Journal of Heat and Mass Transfer 41 (1998) 3373–3385

International Journal of HEAT and MASS TRANSFER

A mixing length model for strongly heated subsonic turbulent boundary layers

R. Meignen*, G. Berthoud

Direction des Réacteurs Nucléaires, Commissariat à l'Energie Atomique de Grenoble, 17 Avenue des Martyrs, 38054 Grenoble Cedex 9, France

Received 7 February 1997; in final form 6 February 1998

Abstract

A model based on the mixing length description is proposed for the prediction of strongly non isothermal subsonic boundary layers. It is validated on a set of experiments involving flows over plates heated up to 1000 K. It is based on the hypothesis that the $u'v'$ profile is not modified by the heating, at least in the internal part of the flow. Regarding the isothermal case, the calculations lead to an appreciable increase of the skin friction (about 30% at 950 K).

Nomenclature

A, B viscous damping distances in mixing lengths
c_f skin friction coefficient
$c_{f,i}$ isothermal skin friction coefficient
C, C_T constants in velocity and temperature log-laws
C_p heat capacity
F_c, F_T functions in (34)
l, l_q mechanical and thermal mixing length
L_T distance from the wall of maximum $\langle v'T' \rangle$
L_u distance from the wall of maximum $\langle u'v' \rangle$
n exponent in the skin friction expression (34)
N factor defined in (15)
P_m, P_t molecular and turbulent Prandtl numbers
q heat flux
R_τ shear stress ratio [see (7)]
Re Reynolds number
Re_m Reynolds number based on δ_m (31)
T temperature
u, v streamwise and crosswise velocity
u^+ dimensionless velocity [see (1) or (11a)]
u_τ friction velocity
U_e external velocity
w wake function (35)
x, y streamwise and crosswise distances
Y_f characteristic distance such that κy_f is a characteristic mixing length
$y^+ = y \cdot u_\tau / v_w$ dimensionless distances
$\langle \cdot \rangle$ mean values (integrated from the wall for physical properties and temporal average for fluctuations).

Greek symbols
δ, δ_T mechanical and thermal thicknesses
δ_m momentum thickness (32)
θ_τ friction temperature
$\kappa = 0.41$ Karmàn constant
μ, v dynamic and kinematic viscosity
Π strength in wake function (36)
ρ density
τ stress
ω characteristic frequency of the turbulent eddies.

Subscripts and superscripts
$'$ fluctuations
$+$ dimensionless quantities (see y^+ for distances such as l^+ or $1/A^+$ and u^+ for velocities)
e external (bulk) properties
m molecular (viscous) properties or momentum properties (Re_m, δ_m)
q or T thermal
t turbulent
s a point at the end of the viscous sublayer in Cebeci's theory
w wall properties
0 isothermal case or equivalent isothermal flow.

* Corresponding author.

0017–9310/98 $19.00
PII: S0017-9310(98)00070-2

1. Introduction

Regarding the very extensive work devoted to turbulent boundary layers (see for example the monographs of Schlichting [1], Kays and Crawford [2] or Cousteix [3]), the case with large wall heat transfer has received very minor attention. In the low wall heating case, i.e. some few tens of degrees, the temperature is just like a neutral transported quantity (Subramania and Antonia [4]): the velocity profile is not modified by the density gradient. On the other side, the compressible turbulent boundary layer is very well documented. Some of its interesting aspects will be used in the following and will then be discussed further. The very small amount of work relative to the case of large wall heating is very surprising, particularly if we consider the possible engineering applications, for example in the nuclear industry. The first experimental work dealing with profile data in subsonic flows with large heating is due to Nicholl [5] ($\Delta T = 100$ K). But the velocity used by Nicholl is very low (2 m s^{-1}), then the buoyancy strongly affects the velocity profile and this work will not be considered here.

The pioneering work in the considered area of strongly heated subsonic turbulent boundary layers is due to Ng [6] and Cheng and Ng [7]. In [6], the air flow velocity is 10.7 m s^{-1} and the plate temperature is about 1250 K. The experiment in [7] involves a 19 m s^{-1} air flow over a 1100 K plate. In these works, it was not noticed a very important effect of the wall heating on the main mechanical characteristics of the flow except a strong reduction of the Reynolds stresses. The classical logarithmic laws for the velocity and temperature are however not valid. In [7] it was suggested that the classical logarithmic law of the wall:

$$u^+ = \frac{u}{u_\tau} = \frac{1}{\kappa}\ln y^+ + C \qquad (1)$$

could be retrieved if the dimensionless distances

$$y^+ = yu_\tau/v \qquad (2)$$

are calculated using the local viscosity, $\kappa = 0.41$ is the Karmán constant, u_τ is the friction velocity and $C = 5$ a constant. In fact this law is retrieved in a quite approximate manner and their velocity profile is better represented with $\kappa = 0.57$ and $C = 8.25$. With this procedure, it is found that the friction velocity u_τ is nearly unchanged. Since u_τ is related to the wall friction τ_w by:

$$\tau_w = \rho_w u_\tau^2 \qquad (3)$$

this means that the wall friction would be reduced, relatively to the isothermal flow, proportionally to the density at the wall. This strong reduction of the wall friction is however in contradiction with the estimations in [6] of the friction coefficient which is found to increase with the wall heating.

Cheng and Ng [7] also found a quite surprising law for the dimensionless temperature:

$$T^+ = \frac{(T_w - T)}{\theta_\tau} = \frac{1}{K_T}\ln y^+ + C_T \qquad (4)$$

with $K_T = 0.8$ and $C_T = 12$ instead of, respectively, 0.45 and 2 for slightly heated flows (Subramania and Antonia [4]). The friction temperature θ_τ is defined from:

$$q_w = \rho_w C_p u_\tau \theta_\tau \qquad (5)$$

where q_w is the wall heat flux. In fact the very high constant C_T obtained here is probably due to a poor determination of q_w (calculated from the thermal layer thickness increase).

In 1992 and 1994, Wardana et al. [8, 9] presented the results of a similar work with a 15 m s^{-1} air flow in a rectangular channel heated on both sides from 610–950 K. They made the same conclusions regarding the mechanical properties of the flow. Eight sets of mean velocity and temperature data are presented and will be used for our calculations. Their characteristics are reported in Table 1 and numbered from (0)–(7). (0) is the isothermal flow, (1)–(4) concern data at the same distance $x = 190$ mm from the beginning of the heating test section, with different wall heatings. (5)–(7) are flows for the largest heating ($q_w = 50$ kW m^{-2}) at different distances x.

No theoretical work on this subject has been found in the literature, and the only descriptive model is the one previously mentioned by Cheng and Ng for the velocity profile (local viscosity for the dimensionless distances). We will present here a model for such strongly heated subsonic turbulent boundary layers. The work is based on the very fertile mixing length theory and on some hypothesis made from the experimental data analysis.

Unfortunately, working with the Cheng and Ng [7] data is difficult because most of them are given using their dimensionless distances, with the local viscosity. The real velocity profile is given only for one streamwise distance ($x = 69$ mm). But when we tried to deduce the dimensional velocities from the dimensionless data (using the density profiles) we did not succeed in retrieving the actual data for the distance $x = 69$ mm. Then, some of the data seem to be quite contradictory. Furthermore, the shape, in logarithmic scale, of the velocity profile is rather strange, or, at least, different from all known shapes since the curvature in the transition region, from the laminar part to the logarithmic one, is positive. As last, the authors did not measure the heat fluxes and then no complete experimental validation is possible with their data. We present two calculations from [6], numbered (8) and (9), but, again, the validation cannot be complete since we do not know the experimental heat flux. Further experimental validation should be possibly researched with trans-sonic or supersonic flows since most of the hypotheses seem applicable to these flows. This would imply some slight modifications. This work has not been

Table 1
Parameters and results of calculations (0)–(7) : Wardana et al. [8, 9], (8)–(10) : Ng. [6]

No.	$q_{w,exp}$	V (m s^{-1})	x (mm)	T_w (K)	q_w (kW m^{-2})	u_τ (m s^{-1})	K	P_t	A^+	$\tau_w/\tau_{w,i}$ [1]	c_f (x 10^{-3}) [2]	δ_m (mm) [3]	$Re_{m,e}$
(0)	isoth.	15	190	300	—	0.69	0.42	—	26	1	4.2	1.42	1350
(1)	[20]	15	190	610	18.5	1	0.45	0.57	15.3	1.03	4.42	1.23	1180
(2)	[30.8]	15	190	790	32.1	1.24	0.52	0.62	14.3	1.22	4.98	1.20	1160
(3)	[36.8]	15	190	860	38.5	1.36	0.56	0.67	14.2	1.35	5.37	1	980
(4)	[50]	15	190	950	46.5	1.45	0.58	0.66	13.7	1.39	5.52	1.04	1050
(5)	[50]	15	140	950	47.7	1.41	0.55	0.60	13.1	1.32	5.22	1.15	1130
(6)	[50]	15	90	900	45.6	1.37	0.54	0.56	13.3	1.31	5.28	1.19	1170
(7)	[50]	15	40	840	48.2	1.27	0.49	0.38	12.5	1.20	4.79	1.23	1210
(8)	?	10.7	150	1250	51	1.205	0.66	0.78	11.3	1.45	6.3	1.11	774
(9)	?	10.7	100	1250	57	1.2	0.64	0.62	10.8	1.44	6.08	1.13	766
(10)	isoth.	10.7	150	300	—	0.49	0.42	—	26	1	4.06	2.04	1385

[1] Ratio of the wall shear stress on the wall shear stress for the isothermal experiment of Wardana et al.
[2] Friction coefficient.
[3] Momentum thickness, see eqn (32).
[4] Reynolds number based on momentum thickness and external properties, see eqn (31).

done because it did not enter in the frame of our project where only subsonic flows are encountered.

The major hypothesis of the present model comes from the experimental observation that the density has not a very great influence on the mechanical fluctuations. In particular, the $\langle u'v' \rangle$ fluctuations are only slightly influenced by the density. This results in a strong reduction of the Reynolds stresses $-\rho\langle u'v' \rangle$ due to the strong reduction of the density near the heated wall. Concerning, the energy equation, we will use the fact that, always from the experiments, the $\langle T' \rangle$[1] fluctuations approximately depends on $(T_w - T_e)$ and the thermal layer thickness. None of the authors gives $\langle v'T' \rangle$ data, and then we make the hypothesis (to be verified) that these $\langle v'T' \rangle$ fluctuations can be extrapolated from $\langle u'v' \rangle$ and $\langle T' \rangle$. We will see that the uncertainty relative to this point has little influence on the velocity profile. The wall heat fluxes that we calculate are in good accordance with the experimental ones and this gives credit to our hypothesis.

2. Momentum and energy equations

In turbulent boundary layer calculations, a usual hypothesis is that the friction and the heat flux are constant over the layer (at least in the viscous and logarithmic parts):

$$\tau = \tau_w = \tau_m + \tau_t \tag{6a}$$

[1] We use the notation $\langle T' \rangle$ for the temperature fluctuations i.e. $\langle T' \rangle \equiv \langle T'^2 \rangle)^{1/2}$.

$$q = q_w = q_m + q_t. \tag{6b}$$

We will now show that, with the experimental evidence that the $\langle u'v' \rangle$ profile is not modified (at least in the logarithmic part of the flow) by the wall heating, the hypothesis of constant friction (6a) has to be modified. If we use a subscript 0 to denote the properties of the flow which would take place without the wall heating, we can write:

$$\frac{\tau_t}{\rho} = -\langle u'v' \rangle = \frac{\tau_{t,0}}{\rho_0} \leqslant \frac{\tau_{w,0}}{\rho_0} = u_{\tau,0}^2. \tag{7}$$

We will note L_u the point along y of maximum turbulent stress. At this point, the viscous component is very small. It follows that the heated maximum turbulent stress is:

$$\tau_{t,L_u} = \rho_{L_u} u_{\tau,0}^2. \tag{7a}$$

Then (6a) leads to:

$$\rho_w u_\tau^2 = \rho_{L_u} u_{\tau,0}^2. \tag{6a$'$}$$

This relation is not necessarily valid (*a priori*), and the equation of constant shear stress (6a) might be a too strong hypothesis.

In order to have an equation similar to (6a), and then to proceed to a similar treatment (i.e. a mixing length model), we propose to scale the turbulent shear stress with the following dimensionless number:

$$R_\tau = \left(\frac{\rho_w}{\varepsilon_{L_u}}\right)\left(\frac{u_\tau}{u_{\tau,0}}\right)^2.$$

Out of the laminar part of the flow, we have:

$$\tau_w = \rho_w u_\tau^2 = \rho_w u_\tau^2 \cdot \frac{\rho_{L_u} u_{\tau;0}^2}{\rho_{L_u} u_{\tau;0}^2}$$

$$\tau_w = R_\tau \cdot \rho_{L_u} u_{\tau;0}^2 \tau_w = R_\tau \cdot \tau_{t;L_u}.$$

With the hypothesis of constant shear stress in the logarithmic part of the flow, we have:

$$\tau_w = R_\tau \cdot \tau_t.$$

Now, taking account of the laminar part, the momentum equation will then be written:

$$\tau_w = \tau_m + R_\tau \tau_t. \tag{8a}$$

Close to the wall, the turbulent stress is very small and (8a) is obvious. Far from the wall, the molecular stress is very small and (8a) is verified if, this is our hypothesis (7), the turbulent stress is constant, equal to $\rho_{L_u}\langle u'v'\rangle_{\text{unheated}}$, leading to a logarithmic part of the flow.

Now considering the heat flux equation, the difficulty comes from the fact that the $\langle v'T'\rangle$ correlations are not given neither by Wardana et al. nor Ng. However, Wardana et al. found that the temperature fluctuations have nearly always the same profile shape, and are scaled by the wall temperature and the thermal layer thickness (see Fig. 10 of Wardana et al. [8]). If we postulate that the velocity fluctuations u' and the temperature fluctuations T' are well correlated, as shown by compressible boundary layer data, we can suppose that the Reynolds analogy still holds when the wall is strongly heated. We will then make the hypothesis that the turbulent heat flux has also to be scaled by R_τ, and the energy equation has to be replaced by:

$$q_w = q_m + R_\tau q_t. \tag{8b}$$

Now, the turbulent shear stress and heat flux will be expressed in terms of the turbulent viscosity and conductivity concepts:

$$-\langle u'v'\rangle = l^2 \left|\frac{du}{dy}\right|^2 \tag{9a}$$

$$-\langle v'T'\rangle = l l_q \left|\frac{du}{dy}\right| \frac{dT}{dy} \tag{9b}$$

where l and l_q are the mechanical and thermal mixing lengths. We obtain the two following equations:

$$\tau_w = \left(\mu + R_\tau \rho l^2 \frac{du}{dy}\right)\frac{du}{dy} \tag{10a}$$

$$q_w = \left(\frac{\mu C_p}{P_m} + R_\tau \rho C_p l l_q \frac{du}{dy}\right)\frac{dT}{dy}. \tag{10b}$$

P_m $(=\mu C_p/k)$, the molecular Prandtl number, is approximately constant around 0.7 for air, whatever the temperature. The variables will be made dimensionless with wall properties by dividing:

(10a) by $\tau_w = \rho_w u_\tau^2$

(10b) by $q_w = \rho_w C_p u_\tau \theta_\tau$.

Note that the heat capacity will be considered constant, although it actually varies by about 10% from 300–1000 K.

Similarly to the compressible case, the density can be removed from the turbulent part of (10) if we define the dimensionless velocity and temperature as (Van Driest density weighted transformations):

$$du^+ = \frac{1}{u_\tau}\sqrt{\frac{\rho}{\rho_p}}\,du \tag{11a}$$

$$dT^+ = \frac{1}{\theta_\tau}\sqrt{\frac{\rho}{\rho_p}}\,dT \tag{11b}$$

and with the dimensionless distances defined as:

$$y^+ = y u_\tau/v_w \tag{12}$$

we obtain the following two equations:

$$1 = \left(\left(\frac{v}{v_w}\right)\left(\frac{\rho}{\rho_w}\right)^{1/2} + R_\tau l^{+2}\frac{du^+}{dy^+}\right)\frac{du^+}{dy^+} \tag{13a}$$

$$1 = \left(\frac{1}{P_m}\left(\frac{v}{v_w}\right)\left(\frac{\rho}{\rho_w}\right)^{1/2} + R_\tau l^+ l_q^+ \frac{du^+}{dy^+}\right)\frac{dT^+}{dy^+} \tag{13b}$$

which are written:

$$\frac{du^+}{dy^+} = \frac{-1+\sqrt{1+4R_\tau l^{+2}/N^2}}{2R_\tau l^{+2}/N} \tag{14a}$$

$$\frac{dT^+}{dy^+} = \frac{1}{\dfrac{N}{P_m} + R_\tau l^+ l_q^+ \dfrac{du^+}{dy^+}} \tag{14b}$$

with:

$$N = \frac{v}{v_w}\left(\frac{\rho}{\rho_w}\right)^{1/2}. \tag{15}$$

Numerical integration of (14) is easy, but we see that it depends on the local viscosity and density of the fluid through the factor N.

3. Mixing length expressions

The mixing length l^+ in (14) is derived from an analogy due to Van Driest with the Stokes problem of a viscous fluid on an oscillating wall (see for example Cebeci [10, 11]). The Prandtl expression for the mixing length $l = \kappa y$ is multiplied by a damping function due to the viscous dissipation in the wall vicinity. We suppose that the Kármán constant κ is not modified by the heating, as for the compressible layers.

Consider then the inverse Stokes problem of a viscous isothermal fluid with an oscillating motion of the form:

$$u = u_0 \cos(\omega t + \phi)$$

then it is easy to show that, close to a fixed wall, the velocity will decrease as:

$$u = u_0(1-e^{-y/A})\cos(\omega t+\psi)$$

where

$$A = (2\nu/\omega)^{1/2}$$

is the damping length.

On analogy, since the u' and v' fluctuations are strongly correlated, we can assume that the damping of $\langle u'v'\rangle$ is of the form $(1-e^{-y/A})^2$. The Prandtl mixing length was then extended in the viscous layer by multiplication with $(1-e^{-y/A})$. Then we have

$$l = (1-e^{-y/A})\kappa y. \quad (16)$$

The turbulent flow in boundary layers does not exhibit only one oscillating frequency but Van Driest has shown that, in dimensionless form, the damping length for the isothermal turbulent boundary layer was a constant:

$$A^+ = Au_\tau/\nu = A(\tau_w/\rho)^{1/2}/\nu = (2\tau_w/\omega\nu\rho)^{1/2}$$

$$A^+ \sim 26.$$

The problem has been extended by Cebeci for various different types of boundary layers, including the cases of compressible flows (slightly) heated flows or flows with pressure gradient. We will now extend his theory for the present case of highly heated flow, in the light of the experimental results discussed before. Following Cebeci, we make the variable change:

$$\mathrm{d}y = \mu\,\mathrm{d}z$$

and then the momentum equation, in the vicinity of the wall becomes:

$$\frac{\partial u}{\partial t} = \frac{1}{\rho\mu}\frac{\partial^2 u}{\partial z^2}.$$

This variable change is made because the product $\rho\mu$ is far less sensitive to the temperature than ρ and μ alone. Then we can integrate this equation with a mean value of $\rho\mu$ denoted $\langle\rho\mu\rangle$. We then have in the case of one frequency:

$$u = u_0(1-e^{-y/A})\cos(\omega t)$$

with

$$A = (2/\langle\rho\mu\rangle\omega)^{1/2}/\langle 1/\mu\rangle.$$

It is also easily verified that, close to the wall, we have

$$\langle\nu\rangle \sim 1/(\langle 1/\mu\rangle\langle\rho\mu\rangle)$$

then:

$$A = (2\langle\nu\rangle/\omega)^{1/2}$$

and

$$y/A = (\omega/2\langle\nu\rangle)^{1/2}y = (\omega\nu^2/2\langle\nu\rangle)^{1/2}y^+/u_\tau.$$

In a first attempt, we made the hypothesis, with Cebeci [11], that the viscous damping verifies the relation:

$$(2/\omega\langle\nu\rangle)^{1/2} \sim 26/(\tau_s/\rho_s)^{1/2}$$

where the subscript s denotes a point at the end of the viscous layer. In Cebeci's theory this point is such that $y_s^+ = 11.8$. But, as we have already said, due to the change of physical properties near the heated wall, the total shear stress is not constant in the layer and, at the beginning of the logarithmic layer, the shear stress is different from the wall shear stress by the factor $1/R_\tau$, and then the model of Cebeci should lead to:

$$(\tau_s/\rho_s) = (\tau_w/\rho_w)(\rho_w/\rho_s)/R_\tau$$
$$= u_\tau^2(\rho_w/\rho_s)/R_\tau.$$

It follows that an expression for the damping constant A^+ would be:

$$A^+ = 26\langle\nu\rangle/\nu_w(\rho_s/\rho_w)^{1/2}R_\tau.$$

But this formula does not give satisfactory results and can not be used to predict adequately the velocity and temperature profiles.

Another expression for A^+ is obtained by analysing the problem in a slightly different way. In the isothermal case, we have:

$$y/A = (\omega/2\nu)^{1/2} \quad y = (\omega\nu/2)^{1/2}y^+/u_\tau.$$

Let us estimate the frequency of the fluctuations by

$$\omega = v'/L_f$$

where L_f is a characteristic length and v' is the crosswise velocity fluctuation. The characteristic value of v' is

$$v' \sim u_\tau$$

and the length L_f can be taken as the mixing length κy_f obtained at some characteristic distance from the wall y_f. Then an expression for ω is:

$$\omega = u_\tau/\kappa y_f$$

and we have:

$$y/A = (u_\tau/2\kappa y_f\nu)^{1/2}y$$
$$= y^+/(2\kappa y_f^+)^{1/2}.$$

Then, if we identify $(2\kappa y_f^+)^{1/2}$ to $A^+ = 26$, we obtain the characteristic dimensionless distance:

$$y_f^+ = 820.$$

This means that the frequency ω is characteristic of the greatest eddies since $y^+ = 820$ corresponds approximately to the dimensionless distance of the wake of the boundary layer (i.e. where the mixing length becomes constant).

In the heated case, we then propose to consider that the characteristic fluctuations leading to the determination of A^+ should be primarily influenced by the bulk flow properties. This is also justified by the fact that all the fluctuating quantities does not seem to undergo the influence of the temperature gradients, as observed in the various experiments. Then, if we use again the subscript 0 for the hypothetical isothermal flow which would arise if the wall was not heated (same bulk velocity and thickness), we can write:

$\omega = u_{\tau 0}/\kappa y_{\mathrm{f}}$

and then

$$\begin{aligned} y/A &= (u_{\tau 0}/\kappa y_{\mathrm{f}}\langle v\rangle)^{1/2}y \\ &= (u_{\tau 0}^2 v_0/2\kappa y_{\mathrm{f}} u_{\tau 0}\langle v\rangle v_0)^{1/2} y^+ v_{\mathrm{w}}/u_\tau \\ &= (u_{\tau 0}/u_\tau)(v_{\mathrm{p}}^2/\langle v\rangle v_0)^{1/2} y^+/(2\kappa y_{\mathrm{f}}^{+0})^{1/2} \\ &= y^+/A^+. \end{aligned}$$

Here, the notation y_{f}^{+0} represents the dimensionless distance with the isothermal flow (*i.e.* $y_{\mathrm{f}}^{+0} = y_{\mathrm{f}} u_{\tau 0}/v_0$). It follows an expression for the constant A^+ if we identify $(2\kappa y_{\mathrm{f}}^{+0})^{1/2}$ with 26:

$$A^+ = 26(u_\tau/u_{\tau 0})(\langle v\rangle v_0/v_{\mathrm{p}}^2)^{1/2}. \tag{17}$$

The problem with (17) comes from the calculation of the average viscosity. In our calculations, the best results are obtained when viscosity is averaged as:

$$\langle v\rangle = \frac{1}{L_{\mathrm{u}}^2}\int_0^{L_{\mathrm{u}}} vy\,\mathrm{d}y$$

where L_{u} is the point of maximum turbulent stress where is also calculated the ratio R_τ. The form of the averaging was dictated from the momentum equation: the curvature of the velocity is more important near L_{u} than near the wall.

The case of the thermal mixing length is more delicate. It is related to the thermal fluctuations damping in $\langle v'T'\rangle$. Cebeci had made the hypothesis that the damping of T' was of thermal nature. Then the thermal mixing length is:

$$l_{\mathrm{q}} = (1-e^{-y/B})\kappa_{\mathrm{q}} y \tag{18}$$

with

$$B = A/P_{\mathrm{m}}. \tag{19}$$

κ_{q} is analogous to the slightly heated case, and we have

$$\kappa_{\mathrm{q}} = \kappa/P_{\mathrm{t}}. \tag{20}$$

This expression defines the turbulent Prandtl number P_{t}.

4. Turbulent Prandtl number

In this section, we will propose an interpretation of the turbulent Prandtl number. For a given experiment, we will see that P_{t} is slowly varying along the plate, increasing with the thermal layer thickness δ_{T}. We suspect it to be due to the fact that the $\langle T'\rangle$ profile and then the $\langle v'T'\rangle$ profile varies with the thermal thickness whereas $\langle u'v'\rangle$ varies with the mechanical thickness.

The thermal fluctuations are transported by the mechanical ones. But it is also clear from the experiments that the general shape of the profiles of the $\langle T'\rangle$ fluctuations is mainly a function of the thermal layer thickness. Then, if the thermal layer is thin relatively to the mechanical one, the thermal fluctuations should be poorly developed whereas the thermal fluctuations should attain their maximum when they are in coincidence with the mechanical fluctuations. In a first approach, we will suppose that the turbulent Prandtl number is constant in the lateral direction and that it can be interpreted as a marker of the coincidence of the mechanical and thermal fluctuations.

As we have no experimental information for $\langle v'T'\rangle$ we made the hypothesis that the $\langle v'T'\rangle$ profile has a similar shape as the $\langle T'\rangle$ profile, or at least that their maximum are obtained for the same value of y. From all the experimental results, we found that $\langle u'v'\rangle/U_{\mathrm{e}}^2$ have similar profiles when plotted vs. y/δ. δ is the mechanical boundary layer thickness. They also found that, with a good approximation $\langle T'\rangle/(T_{\mathrm{w}}-T_{\mathrm{e}})$ varies slightly, but only in amplitude when plotted vs. y/δ_{T}. Then we can write:

$$\langle u'v'\rangle = U_{\mathrm{e}}^2 f(y/\delta) \tag{21a}$$

$$\langle T'\rangle = C_1(T_{\mathrm{w}}-T_{\mathrm{e}})g(y/\delta_{\mathrm{T}}) \tag{21b}$$

with C_1 a constant slowly varying around 1. We also find from the experiments of Wardana et al., that the maximum of $\langle T'\rangle$ approximately lies at $L_{\mathrm{T}} = \delta_{\mathrm{T}}/12$. Then we make the hypothesis that L_{T} is also approximately the point of maximum $\langle v'T'\rangle$.

Now, since the temperature fluctuations are transported by the velocity fluctuations, the amplitude of $\langle T'\rangle$ and $\langle v'T'\rangle$ will attain a maximum value when there is coincidence between the $\langle u'v'\rangle$ and $\langle v'T'\rangle$ profile, i.e., when $L_{\mathrm{T}} = L_{\mathrm{u}}$. If $L_{\mathrm{T}} < L_{\mathrm{u}}$, $\langle v'T'\rangle$ is not completely developed and we suppose that the amplitude of $\langle v'T'\rangle$ is proportional to the value of $\langle u'v'\rangle$ at the point L_{T}. So if we note for a given test (see Fig. 1)

- a_i the maximum amplitude of $\langle T'\rangle/(T_{\mathrm{w}}-T_{\mathrm{e}})$,
- b_i the amplitude of $\langle u'v'\rangle/U_{\mathrm{e}}^2$ at that point,
- $L_{\mathrm{T}i}$ the corresponding length for the maximum of $\langle T'\rangle/(T_{\mathrm{w}}-T_{\mathrm{e}})$,

then we make the hypothesis that the amplitudes are such that (see Fig. 1):

$$a_2/a_1 = b_2/b_1 = L_{\mathrm{T}2}/L_{\mathrm{T}1}.$$

The second equality follows from the linear approximation in the ascending part of $\langle u'v'\rangle$. Finally, we make the hypothesis that the turbulent Prandtl number reflects the fact that $\langle v'T'\rangle$ is not completely developed and that P_{t} is the ratio between the maximum possible value of $\langle v'T'\rangle$ when the Reynolds analogy is complete (i.e. $L_{\mathrm{T}} = L_{\mathrm{u}}$) to its actual value.

Then we finally obtain:

$$P_{\mathrm{t}} = L_{\mathrm{T}}/L_{\mathrm{u}} = \delta_{\mathrm{T}}/(12L_{\mathrm{u}}). \tag{22}$$

Equation (22) has been obtained after some probably questionable hypotheses. However, as we will see further, its accuracy regarding the calculated experiments is rather good (its influence is easily detected since P_{t} is proportional to the slope of the logarithmic part of the temperature profile).

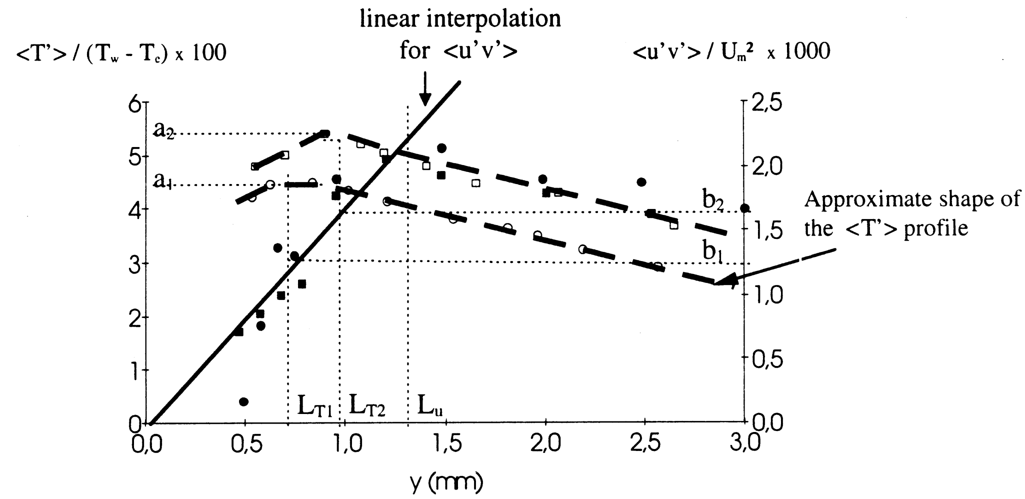

Fig. 1. Some experimental values of $\langle u'v'\rangle$ and $\langle T'\rangle$ for two tests with similar thickness δ. → Open symbols: $\langle T'\rangle/(T_w - T_e)$ ($\times 100$); closed symbols $\langle u'v'\rangle/U_m^2$ ($\times 1000$); → squares: $q_w = 30.8$ kW m^{-2}, circles; $q_w = 50$ kW m^{-2}. → a_1 and a_2 are the maxima of $\langle T'\rangle/(T_w - T_e)$, located at the length L_{T1} and L_{T2}. → L_u represents the location of $\langle u'v'\rangle_{max}$. → b_1 and b_2 are the values of $\langle u'v'\rangle$, at the positions L_{T1} and L_{T2}.

5. Point of maximum turbulent stresses

We will now evaluate the point L_u of maximum turbulent stress which has been shown to depend only on δ. Since the profile of $\langle u'v'\rangle$ does not change with the wall temperature, the point L_u of maximum $\langle u'v'\rangle$ in (7) and (22) can be evaluated from the isothermal expression of the turbulent stresses (Tennekes and Lumley, [12])

$$\frac{-\langle u'v'\rangle}{u_{\tau,0}^2} + \frac{du^{+,0}}{dy^{+,0}} + \frac{y^{+,0}}{\delta^{+,0}}, -1 = 0. \tag{23}$$

We note with the superscript $+,0$ the isothermal flow which would take place without the wall heating. Then the point of maximum turbulent stress in the isothermal flow (and then in the heated flow) is found by derivation of (23):

$$\frac{d^2u^{+,0}}{d(y^{+,0})^2} + \frac{1}{\delta^{+,0}} = 0.$$

The second derivative of the velocity is found by deriving the isothermal expression of (9a):

$$\frac{du^{+,0}}{dy^{+,0}} = \frac{1+\sqrt{1+4(1^{+,0})^2}}{2(1^{+,0})^2}$$

with the mixing length:

$$1^{+,0} = \kappa y^{+,0}(1-e^{y^{+,0}/26}).$$

This leads to an implicit equation which has the following approximation:

$$\frac{1^{+,0}}{y^{+,0}} + \frac{y^{+,0}}{26}e^{y^{+,0}/26} = \frac{(1^{+,0})^2}{\delta^{+,0}}. \tag{24}$$

The solution is in very good agreement with the experimental data of Wardana et al.

6. Results

We have first to precise how the dimensionless experimental data u^+ and T^+ were obtained from (11). The expression

$$dT^+ = \frac{1}{\theta_\tau}\sqrt{\frac{\rho}{\rho_w}}dT \tag{11b}$$

is easy to integrate if we suppose that air is a perfect gas. We obtain:

$$T^+ = \frac{2}{\theta_\tau T_w}\left(1-\left(\frac{T}{T_w}\right)^{1/2}\right). \tag{25}$$

An analytical integration of

$$du^+ = \frac{1}{u_\tau}\sqrt{\frac{\rho}{\rho_w}}du \tag{11a}$$

is only possible if we suppose a relation between u^+ and T^+. We made a numerical integration with interpolation of the temperature at each experimental point (y, u).

Coming back to equations (14a,b), we see that close to the wall, when $y^+ \to 0$, then $l^+ \to 0$, and we have the tendency (with $(1+\varepsilon)^n = 1+n\varepsilon$):

$$\frac{du^+}{dy^+} \underset{y^+\to 0}{\to} \frac{1}{N}. \tag{26a}$$

The thermal dimensionless profile is also modified since we have:

$$\frac{dT^+}{dy^+} \underset{y^+\to 0}{\to} \frac{P_m}{N}. \tag{26b}$$

As N varies very quickly near the wall, the profiles near the wall are not linear but have a positive curvature. However we always have the classical relation:

$$T^+ \underset{y^+\to 0}{=} P_m u^+. \tag{27}$$

Out of the viscous sublayer, when l^+ is large, we find the tendency:

$$\frac{du^+}{dy^+} \underset{y^+\to\infty}{\to} \frac{1}{Ky^+} \tag{28a}$$

$$\frac{dT^+}{dy^+} \underset{y^+\to\infty}{\to} \frac{P_t}{Ky^+} \tag{28b}$$

where K is an equivalent Karmán constant:

$$K = R_\tau^{1/2}\kappa. \tag{29}$$

We obtain a logarithmic behaviour similar to the isothermal case, but with a different slope, due to the reduction of the Reynolds stresses.

The Fig. 2 shows the sensitivity of the parameters A^+ and R_τ on the calculations. The calculation with black circles is made for arbitrary parameters chosen around the typical values that have been found for the experiments of Wardana et al. and Ng. The one with empty circles shows the sensitivity when A^+ is increased by 1.4. The flow becomes logarithmic for a larger distance y. In this part of the flow, the values of u^+ and T^+ are higher but the slope is unchanged. The laminar part of the flow is not modified. The curves with empty squares show the

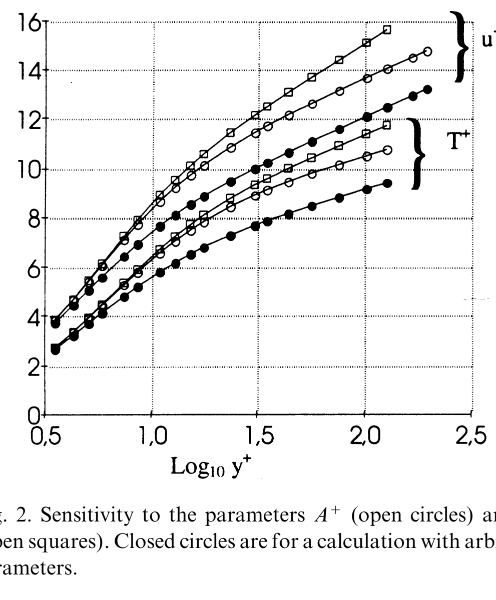

Fig. 2. Sensitivity to the parameters A^+ (open circles) and R_τ (open squares). Closed circles are for a calculation with arbitrary parameters.

influence when R_τ is multiplied by 1.4. The effect is to modify the slope of the logarithmic part of the curve as is expected from eqns (28) and (29). A modification of B^+ would have the same effect than A^+ but mainly on the thermal curve, whereas the effect of the turbulent Prandtl number is also clearly seen with the slope of the logarithmic part of the thermal curve [through (28b)].

Then the effect of each of these parameters can be detected separately so that any discrepancy in the results can be understood. The major uncertainties of the model come from the evaluations of the physical properties (c_p, $\langle v\rangle$). In the present calculations the heat capacity and the mean viscosity are evaluated at the point of maximum shear stress (as for R_τ). In dimensionless form, we found that this point is always greater than A^+ (i.e. $L_u^+ > A^+$) so that the viscosity is averaged over the main part of the viscous damping. The uncertainty for these two parameters is only about 10%.

We will now compare the results of our model with the experiments of Wardana et al. [8, 9] and Ng [6]. The results of the calculations for the different experiments are found in Fig. 3 and in Table 1. These calculations consist in a numerical integration of eqns (14):

$$\frac{du^+}{dy^+} = \frac{-1+\sqrt{1+4R_\tau l^{+2}/N^2}}{2R_\tau l^{+2}/N} \tag{14a}$$

$$\frac{dT^+}{dy^+} = \frac{1}{\dfrac{N}{P_m} + R_\tau l^+ l_q^+ \dfrac{du^+}{dy^+}} \tag{14b}$$

together with expressions (16)–(20), (22) and the solution of (23). We adjust the values of the friction velocity and the wall heating in order to have the best fit with the experimental values of the velocity and the temperature profiles [or more precisely with (25) and the numerical integration of (11a)].

We see in Fig. 3 that the fitting is in general rather good, especially in the logarithmic part. It is less satisfying in the viscous part and the model might underpredict the velocity and temperature in this zone. However, the experimental precision should be less good in this region due to the wall effects on the measurements (LDV technology for the velocity). This difficulty is clearly seen with the isothermal test (0) on Fig. 7. The profiles for the experiment of Ng are a bit less well presented. The turbulent Prandtl number might be a bit overestimated. It is then possible to suspect some differences between channel flows as in Wardana et al. and a plate flows as in Ng. However, the general tendency is rather satisfying.

The calculated friction velocities are strongly augmented by the wall heating since in the isothermal case, u_τ is approximately 0.7 m s^{-1}. With the method proposed by Cheng and Ng (local viscosity used for dimensionless distances and classical adimensions for the velocity and temperature), u_τ is only slightly increased. Then, since we

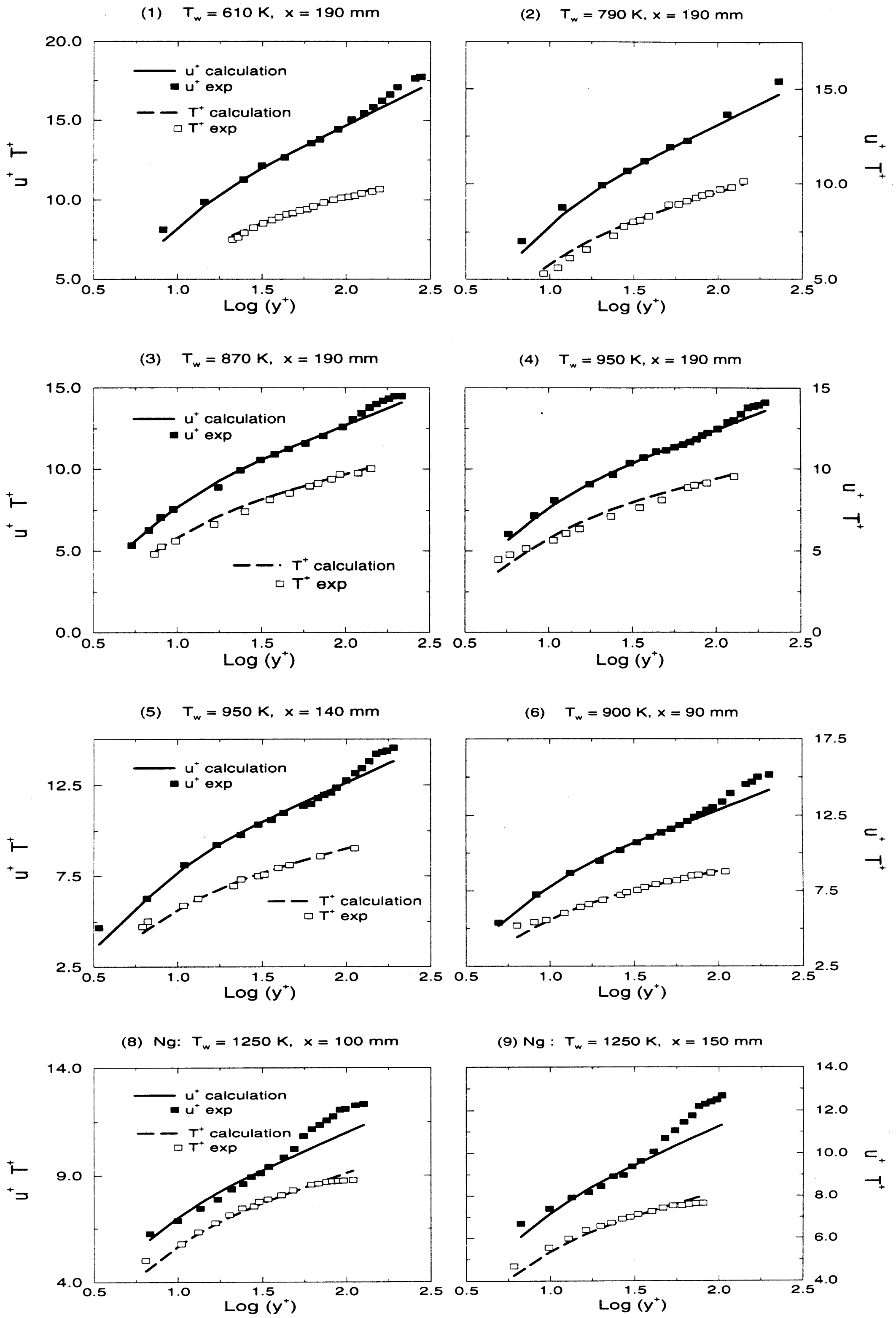

Fig. 3. u^+ and T^+ profiles for the experiments (1)–(9) with parameters listed in Table 1.

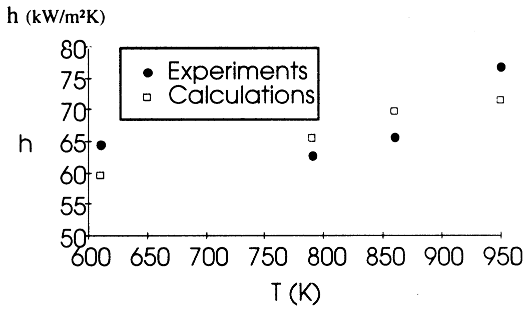

Fig. 4. Heat transfer coefficient h for the four experiments at 190 mm of Wardana et al.

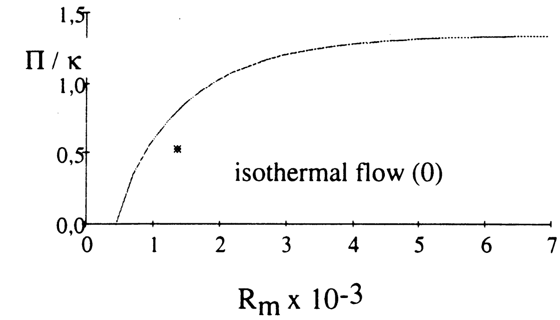

Fig. 6. Fitting formula (36) for Π/κ.

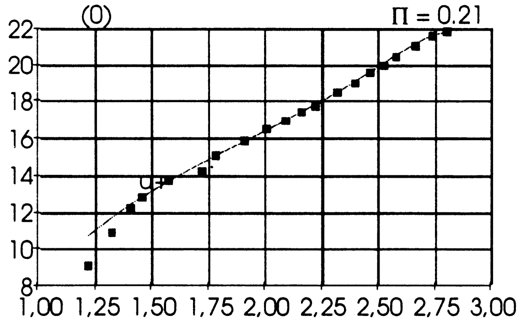

Fig. 7. Isothermal flow (0) velocity profile using the mixing length model and the law of the wake (35).

have $\tau_w = \rho_w u_\tau^2$, they obtain a wall friction which highly decreases with wall heating. On the contrary, we find a wall friction slightly increasing with wall temperature (about 30% at 1000 K). Since the fitting is quite good close to the wall (it seems furthermore to slightly underestimate the velocity in this region, and then the friction), we can expect that our results are in better agreement with experiments than those obtained with the Cheng and Ng method which is only based on a fitting in the logarithmic part of the flow (and which has no theoretical backgrounds). Note also that, in Ng thesis [6], the heating was estimated to increase appreciably the friction coefficient.

The values obtained for the wall heat flux are very close to the experimental one. The heat flux is in general well estimated with an error lower than 10%. The heat transfer coefficient, defined by $h = q_w/(T_w - T_e)$ is compared with the experimental one in Fig. 4. It seems to increase linearly with the wall heating.

Modifications of the turbulent Prandtl number P_t, and then the imprecision on the knowledge $\langle v'T' \rangle$ have been found to have a little influence on the velocity profile. It only affects the quality of the fitting of the temperature data, and the calculated value of q_w. Note that the modelling of this parameter P_t, which was rather delicate to obtain, seems to be particularly satisfying in its predictions since the slope of the logarithmic part of the thermal data is well calculatedd [eqn (28b)]. In particular, the thermal field of the test (6) and (7) are well reproduced although their thermal layers are very thin (they are only 90 and 40 mm downstream from the beginning of the heated plate). The calculation of a turbulent Prandtl number of 0.36 is in very good agreement with the experimental data (the classical value is around 0.85).

Our model seems able to calculate with a good accuracy the velocity and temperature profiles of a subsonic turbulent boundary layer submitted to a high wall heat-

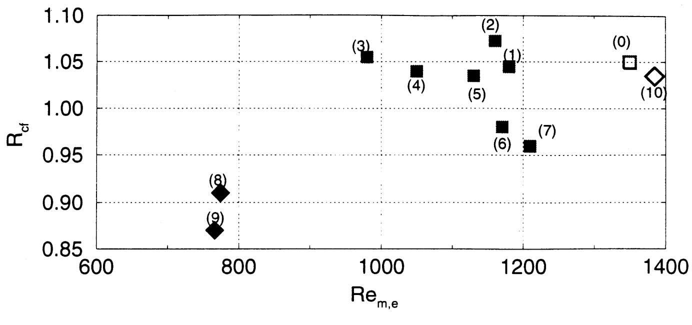

Fig. 5. Ratio $R_{cf} = c_f F_c / c_{f,i}(Re_{m,e} F_T)$ with $n = 2.5$ (i) as in Table 1. Squares: Wardana et al. data, diamonds: Ng data; empty symbols: isothermal tests.

ing. Little uncertainties subsist on the temperature profile due to uncertainties on the knowledge on the $\langle v'T' \rangle$ correlation. However, they affect only very slightly the velocity profile.

7. Possible skin friction correlations

We will now propose a possible correlation for the skin friction coefficient c_f. In the non-isothermal case, it is given by:

$$c_f = 2\frac{\rho_w}{\rho_e}\left(\frac{u_\tau}{U_e}\right)^2. \quad (29)$$

Of course we do not have enough experimental data to obtain statistically a precise formulation, and these must be taken as a first attempt towards a correlation.

The first difficulty for this attempt is that the Reynolds numbers of the considered flows are very low, and then the isothermal correlations are not very accurate. Several correlations exist but they all underpredict the skin friction when the Reynolds number is too low. Of these correlations, we will use the formula recommended by Huang et al. [13], the Karmán–Schoenherr correlation:

$$c_{f,i} = (17.08x^2 + 25.11x + 6.012)^{-1}$$
$$x = \log_{10} Re_m. \quad (30)$$

The Reynolds number Re_m is based on the momentum thickness δ_m:

$$Re_m = U_e \delta_m / \nu \quad (31)$$

$$\delta_m = \int_0^\delta \frac{\rho u}{\rho U_e}\left(1 - \frac{u}{U_e}\right) dy \quad (32)$$

(30) gives slightly better results than the classical formula: $c_f = 0.0172\, Re_m^{0.2}$. We find for the isothermal flow a friction velocity higher by 2.5% (5% regarding c_f) than the value given by (30) (δ_m is calculated by a numerical integration with the experimental data points). Then the discrepancy is acceptable.

For the non isothermal case the Reynolds number has to be calculated with a particular value of the viscosity. We can define the wall, external, and composite Reynolds numbers:

$$Re_{m,w} = U_{max}\delta_m/\nu_w \quad (33a)$$

$$Re_{m,e} = U_{max}\delta_m/\nu_e \quad (33b)$$

$$Re_{m,c} = \rho_e U_{max}\delta_m/\mu_w \quad (33c)$$

and try to find correlations using these Reynolds number.

The first possibility is simply to use (30) with one of the Reynolds number. The best result is obtained with the composite Reynolds number (33b), as Huang et al. [13] suggested for the compressible case.

We can also postulate, as for compressible boundary layers, that the skin friction can be expressed from the isothermal correlation in the following form (Spalding and Chi [14]):

$$c_f F_c = c_{f,i}(Re_{m,e} F_T) \quad (34a)$$

where F_c is a function of the velocity profile, and F_T a function of the temperature profile defined by:

$$F_c = u^+_{max} u_\tau / U_{max} \quad (34b)$$

$$F_T = (T_e/T_w)^n \quad (34c)$$

F_c is independent on u_τ [see (11a)], and is equal to one for isothermal flows. The ratio

$$R = c_f F_c / c_{f,i}(Re_{m,e} F_T)$$

is plotted on the Fig. 5 vs. the Reynolds number $Re_{m,e}$ when we use $n = 2.5$. This value for n gives an average ratio $R = 1.05$ for the isothermal case. This choice for n is due to the fact that (30) underestimate this case with an error of 5%. The discrepancies from the mean value are very small for the tests of Wardana et al. Even at $x = 40$ mm, for the test (7) the discrepancy is only 10% (5% regarding u_τ). The result is less good for the Ng tests. The discrepancy is however only 15%. It is not possible to say at the present stage if the discrepancy for the Ng tests is due to the flow nature (air flow over a flat plate whereas in Wardana et al., it is an air flow in a channel), to the higher temperature or to a very small Reynolds number (c_{f_i} should be strongly underestimated).

We conclude that the formula (34) is, as a first step, rather satisfying and can be used with $n = 2.5$ to estimate the skin friction for turbulent boundary layers with heated walls.

8. The wake of the boundary layer

We have to predict the complete velocity profile, including the wake part of the flow which has not been discussed yet. This part is very important in the calculation of the momentum thickness (and then on $Re_{m,e}$) and on F_c.

For the case of weakly heated turbulent boundary layers, several forms have been proposed for the law of the wake, of which the Dean's formula (Subramania and Antonia [4]):

$$u^+ = \frac{u_\tau}{\kappa}\log y^+ + \frac{\Pi}{\kappa} w\left(\frac{y}{\delta}\right)$$

$$\frac{\Pi}{\kappa} w\left(\frac{y}{\delta}\right) = \frac{1}{\kappa}(1+6\Pi)(y/\delta)^2 - \frac{1}{\kappa}(1+4\Pi)(y/\delta)^3. \quad (35)$$

A fitting formula for Π is:

$$\Pi = 0.55(1 - \exp(-0.24\sqrt{z} - 0.75z)) \quad (36)$$

with

$$z = Re_m 10^{-3} - 0.45.$$

The wake law for temperature is analogous but the strength Π_T is about half of Π. It seems also that the thermal wake appears for larger Reynolds numbers with respect to the mechanical wake (for further details, see Subramania and Antonia [4]). But is obvious that in all the experiments considered here, no thermal wake is detected (see Fig. 3). This might be due to an incomplete development of the thermal layers. However, in the slightly heated case, the thermal wake, when detected, is always less important than the mechanical wake. In all cases, its influence on predictions is probably rather weak, especially for the mechanical properties. Then it can be forgotten until more experimental data are available.

The isothermal flow velocity profile is plotted on Fig. 7 using the classical mixing length model and the law of the wake (35). It is seen that the shape of the law fits very well the experimental data (except again close to the wall). But the calculated strength Π is a little bit smaller than the value predicted by (36) (see Fig. 6).

For the heated case the preceding formulae (35) and (36) are not accurate. It is possible to describe the wake with a slight modification of (35), but, in dimensionless variables y^+u^+, the strength of the wake changes also with the wall temperature and the length x of the heated section.

In fact, an easier way to describe this wake is to remark that it does not seem to be modified by the heating (in u, y variables). Then it is better to use the isothermal description for this part of the flow. This can be done easily because in the logarithmic part of the flow the velocity is higher in the heated flow than for the isothermal flow, as is seen on the Fig. 8. But there is a point where the two profiles merge. Then the procedure can be simply to calculate for each point the velocity with the present model, and the corresponding isothermal flow (with the wake), and to retain the higher value.

9. An integral representation of the velocity profile

It might also be interesting to note that it is possible to represent rather accurately the velocity profile with a simple formula. In isothermal flows, the laminar and logarithmic part can be represented with the so-called Spalding formula [3]:

$$y^+ = u^+ + \frac{1}{E}\left(e^{\kappa u^+} - \sum_{n=0}^{1} \frac{(\kappa u^+)^n}{n!}\right) \tag{37}$$

where κ is the Karmán constant and $E = 10$. Is a constant: we found that this formula was also rather valid provided that:

- the constant κ is replaced by the constant K found in the preceding sections,
- the quantities are made dimensionless using the density weighted transformations (11):

This gives:

$$y^+ = u^+ + \frac{1}{E}\left(e^{\kappa u^+} - \sum_{n=0}^{1} \frac{(\kappa u^+)^n}{n!}\right). \tag{38}$$

An example of application with the flow (4) is shown in Fig. 9.

In this case, we find that the best fit is obtained with a friction velocity which is about 7% higher than the value found with the complete model.

A similar formula can be used for the temperature profile but with a constant E which changes with the Prandtl number. The use of the formula (38) is then not straightforward since it needs the temperature profile and the constant E. However, for a moderate heating and long distances (in which case the Prandtl number is close to its classical value 0.85), the temperature can be guessed with a similar equation to (38) with:

- replaced by T^+
- K replaced by $K_T = K/P_t$
- E replaced by $E_T = 15$.

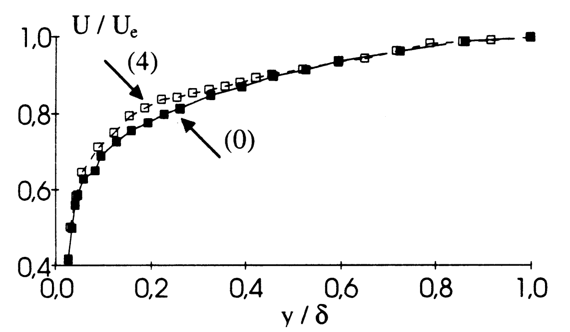

Fig. 8. Velocity profiles for the isothermal flow (0) and the flow (4) with $T_w = 950$ K.

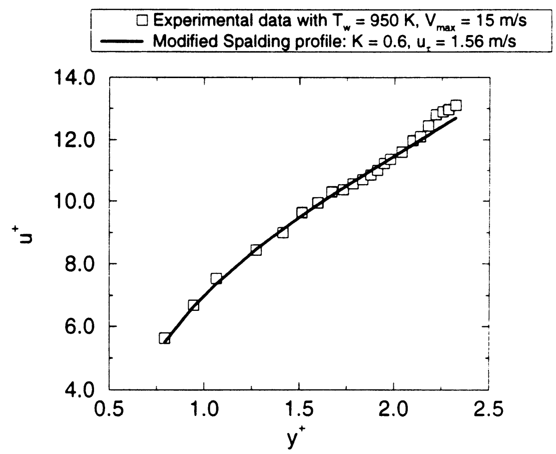

Fig. 9. Application of the modified Spalding formula to the flow (4) with $T_w = 950$ K.

10. Conclusions

The procedure which has been drawn here seems able to describe accurately the velocity and temperature profiles of the highly heated subsonic turbulent boundary layers measured by Wardana et al. [8, 9] and Ng [6]. The model that has been proposed is a modification of the mixing length model used for isothermal or compressible boundary layers. From the isothermal case, the main changes come from the experimental observation that the density gradient does not seem to influence the mechanical fluctuation quantities such as $\langle u'v' \rangle$. This leads to a reduction of the Reynolds stresses, and then to a modification of the slope of the logarithmic part of the profiles. The modification of the turbulent Prandtl number is supposed to be a result of the scaling of the $\langle T' \rangle$ fluctuations with the thermal layer thickness. The damping constant A^+ in the mixing length expression is modified in a different way from the Cebeci analysis for compressible layers. The wake is only very slightly modified from the isothermal case and it is then suggested to use the isothermal theory for this part of the flow.

The model calculates the profiles and the wall heat flux with an accuracy at least equal to the experimental one. A correlation for the skin friction coefficient is proposed [eqn (34)]. At the present stage, further experimental data are required in order to validate or modify the model, especially the skin friction correlation.

The present model is quite simple. We only have two unknowns which are the friction velocity and temperature (i.e. the wall temperature or the wall heat flux). Then, given two data, for example δ and δ_T, or δ and $R_{m,e}$ or $R_{m,e}$ alone with the friction correlation (34), predictions can be obtained by an iterative procedure similar to the one proposed by Huang et al. [13]. For example, suppose that we have the thicknesses δ and δ_T together with the bulk velocity and the wall temperature. The first step is to calculate the isothermal flow that would take place if no heating occurred. This will give $u_{\tau,0}$ which is used in (7), (17) for R_τ and A^+. This also gives the wake part of the flow. Then, given an estimation of u_τ and q_w, we can calculate R_τ, A^+ and P_t, and perform the integration of (14). By comparison of the new calculated values of δ and δ_T (i.e. where the velocity and temperature attains their bulk values), we can re-estimate u_τ and q_w and continue the procedure until convergence.

References

[1] Schlichting H. Boundary Layer Theory. McGraw-Hill, 6th edn, 1968.

[2] Kays WM, Crawford ME. Convective Heat and Mass Transfer. McGraw-Hill, 2nd edn, 1980.

[3] Cousteix J. Turbulence et Couche Limite, ed. CEPADUES. Toulouse, 1989.

[4] Subramanian CS, Antonia RA. Effects of Reynolds number on a slightly heated turbulent boundary layer. International Journal of Heat Mass Transfer 1981;24(11):1833–46.

[5] Nicholl CIH. Some dynamical effects of heat on a turbulent boundary layer. Journal of Fluid Mechanics 1970;40:361–84.

[6] Ng TT. Experimental study of a chemically reacting turbulent boundary layer. Ph.D. thesis, University of California, Berkeley, 1981.

[7] Cheng RK, Ng TT. Some aspects of strongly heated turbulent boundary layer flows. Phys Fluid 1982;25(8):1333–41.

[8] Wardana ING, Ueda T, Mizomoto M. Structures of turbulent two-dimensional channel flow with strongly heated wall. Experiments in Fluids 1992;13:17–25.

[9] Wardana ING, Ueda T, Mizomoto M. Effect of strong wall heating on turbulence statistics of a channel flow. Experiments in Fluids 1994;18:87–94.

[10] Cebeci T. A model for eddy conductivity and turbulent Prandtl number. Journal of Heat Transfer 1973;95:227–34.

[11] Cebeci T. Calculation of compressible turbulent boundary layers with heat and mass transfer. AIAA Journal 1971;9(6):1091–7.

[12] Tennekes H, Lumley HL. A First Course in Turbulence. MIT Press, 1972.

[13] Huang PG, Bradshaw P, Coakley TJ. Skin friction and velocity profile family for compressible turbulent boundary layer. AIAA Journal 1993;31(9):1600–4.

[14] Spalding DB, Chi SW. The drag of compressible turbulent boundary layer on a smooth flat plate with and without heat transfer. Journal of Fluid Mechanics 1963;117–43.